Contents

11

Region-Based Segmentation: Fuzzy Connectedness, Graph Cut and Related Algorithms

Krzysztof Chris Ciesielski and Jayaram K. Udupa

Abstract. In this chapter, we will review the current state of knowledge on region-based digital image segmentation methods. More precisely, we will concentrate on the four families of such algorithms: (i) The leading theme here will be the framework of fuzzy connectedness (FC) methods. (ii) We will also discuss in detail the family of graph cut (GC) methods and their relations to the FC family of algorithms. The GC methodology will be of special importance to our presentation, since we will emphasize the fact that the methods discussed here can be formalized in the language of graphs and graph cuts. The other two families of segmentation algorithms we will discuss consist of (iii) watershed (WS) and (iv) the region growing level set (LS) methods. Examples from medical image segmentation applications with different FC algorithms are also included.

11.1 Introduction and Overview

In this chapter, we will review the current state of knowledge in region-based digital image segmentation methods, with a special emphasis on the fuzzy connectedness family of algorithms. The other image segmentation methods are discussed in the other chapters of this book and we will refer to them only marginally. We will put a special emphasis on the delineation algorithms, that is, the segmentation procedures returning only one Object Of Interest (OOI) at a time rather than multiple objects simultaneously. This will make the presentation clearer, even for the methods that can be easily extended to the multi-object versions.

We will discuss only the region-growing-type delineation algorithms, which in Chapter 1 are referred to as agglomerative or bottom-up algorithms. More precisely, we will concentrate on the four families of such algorithms. The leading theme will be the framework of Fuzzy Connectedness (FC) methods developed since 1996 [1–6], including a slightly different approach to this methodology, as presented in papers [7–9]. For some applications of FC, see also e.g. [10,11]. We will also discuss the family of Graph Cut (GC) methods [12–20] and their relations to the FC family of algorithms. The GC methodology will

be of special importance to our presentation, since we will formalize the FC framework in the language of graphs and graph cuts. The other two families of segmentation algorithms we will discuss consist of Watershed (WS) [21–23] and region growing Level Set (LS) methods from [24, 25].

The common feature of all the presented algorithms is that the object to be segmented by them is indicated (by user, or automatically) by one or more space elements (*spels*) referred to as *seeds*. In addition, if P is an object returned by such an algorithm, then any spel belonging to P is connected to at least one of the seeds indicating this object. The word "connected" indicates, that the topological properties of the image scene play important role in this class of segmentation processes. So, we will proceed with explaining what we mean by the image scene, its topology, as well as the notion of connectedness in this context.

For the rest of this chapter, $\mathfrak{n} \geq 2$ will stand for the dimension of the image we consider. In most medically relevant cases, $\mathfrak{n}$ is either 2 or 3, but a time sequence of 3D images is often considered as a 4D image.

11.1.1 Digital Image Scene

A digital image scene C can be identified with any finite subset of the $\mathfrak{n}$-dimensional Euclidean space $\mathbb{R}^{\mathfrak{n}}$. However, we will concentrate here only on the case most relevant for medical imaging, in which C is of the rectangular form $C_1 \times \cdots \times C_{\mathfrak{n}}$ and each C_i is identified[1] with the set of integers $\{1, \ldots, m_i\}$.

A topology on a scene $\boldsymbol{C} = \langle C, \alpha \rangle$ will be given in terms of adjacency relation α, which intuitively determines which pair of spels $c, d \in C$ is "close enough" to be considered connected. Formally, an adjacency relation α is a binary relation on C, which will be identified with a subset of $C \times C$, that is, spels $c, d \in C$ are α-adjacent, if and only if, $\langle c, d \rangle \in \alpha$. From the theoretical point of view, we need only to assume that the adjacency relation is symmetric (i.e., if c is adjacent to d, then also d is adjacent to c).[2] However, in most medical applications, it is enough to assume that c is adjacent to d when the distance[3] $||c-d||$ between c and d does not exceed some fixed number. In most applications, we use adjacencies like 4-adjacency (for $\mathfrak{n} = 2$) or 6-adjacency (in the Three-dimensional (3D) case), defined as $||c - d|| \leq 1$. Similarly, the 8-adjacency (for $\mathfrak{n} = 2$) and 26-adjacency (in 3D) relations can be defined as $||c - d|| \leq \sqrt{3}$.

[1] This identification of the coordinates of spels with the integer numbers is relevant only for the computer implementations. For theoretical algorithmic discussion, especially for anisotropic images, we will assume that C_i's are the real numbers of appropriate distances.

[2] Usually it is also assumed that α is reflexive (i.e., any spel c is adjacent to itself, $\langle c, c \rangle \in \alpha$), but this assumption is not essential for most considerations.

[3] In the examples, we use the Euclidean distance $|| \cdot ||$. But any other distance notion can be also used here.

The adjacency relation on C translates to the notion of connectivity as follows. A (connected) path p in a subset A of C is any finite sequence $\langle c_1, \ldots, c_k \rangle$ of spels in A such that any consecutive spels c_i, c_{i+1} in p are adjacent. The family of all paths in A is denoted by $\mathbb{P}^A$. Spels c and s are connected in A provided there exists a path $p = \langle c_1, \ldots, c_k \rangle$ in A from c to s, that is, such that $c_1 = c$ and $c_k = s$. The family of all paths in A from c to d is denoted by $\mathbb{P}^A_{cd}$.

11.1.2 Topological and Graph-Theoretical Scene Representations

The topological interpretation of the scene given above is routinely used in the description of many segmentation algorithms. In particular, this is the case for FC, WS, and most of the LS methods. On the other hand, the algorithms like GC use the interpretation of the scene as a directed graph $G = \langle V, E \rangle$, where $V = C$ is the set of vertices (sometimes extended by two additional vertices) and E is the set of edges, which are identified with the set of pairs $\langle c, d \rangle$ from $V = C$ for which c and d are joined by an edge.

Note that if we define E as the set of all adjacent pairs $\langle c, d \rangle$ from C (i.e., when $E = \alpha$), then the graph $G = \langle V, E \rangle$ and the scene $\boldsymbol{C} = \langle C, \alpha \rangle$ are the identical structures (i.e., $G = \boldsymbol{C}$), despite their different interpretations. This forms the basis of the duality between the topological and graph-theoretical view of this structure: any topological scene $\boldsymbol{C} = \langle C, \alpha \rangle$ can be treated as a graph $G = \langle C, \alpha \rangle$ and, conversely any graph $G = \langle V, E \rangle$ can be treated as topological scene $\boldsymbol{C} = \langle V, E \rangle$.

Under this duality, the standard topological and graph theoretical notions fully agree. A path p in C is connected in $\boldsymbol{C} = G$ in a topological sense, if and only if, it is connected in the graph $G = \boldsymbol{C}$. A subset P of C is connected, in a topological sense, in $\boldsymbol{C} = G$, if and only if, it is connected in the graph $G = \boldsymbol{C}$. The symmetry of α translates into the symmetry of the graph $G = \langle C, \alpha \rangle$, and since any edge $\langle c, d \rangle$ in G can be reversed (i.e., if $\langle c, d \rangle$ is in $E = \alpha$, then so is $\langle d, c \rangle$), G can be treated as an undirected graph.

11.1.3 Digital Image

All of the above notions depend only on the geometry of the image scene and are independent of the image intensity function. Here, the image intensity function will be a function f from C into $\mathbb{R}^k$, that is, $f \colon C \to \mathbb{R}^k$. The value $f(c)$ of f at c is a k-dimensional vector of image intensities at spel c. A digital image will be treated as a pair $\langle \boldsymbol{C}, f \rangle$, where $\boldsymbol{C}$ is its scene (treated either as a topological scene or as a related graph) and f is the image intensity. We will often identify the image with its intensity function, that is, without explicitly specifying associated scene adjacency. In case when $k = 1$ we will say that the image is scalar; for $k > 1$ we talk about vectorial images. Mostly, when giving examples, we will confine ourselves to scalar images.

11.1.4 Delineated Objects

Assume that with an image $\langle \boldsymbol{C}, f\rangle$ we have associated an energy function $\boldsymbol{e}$, which for every set $P \subset C$ associates its energy value $\boldsymbol{e}(P) \in \mathbb{R}$. Assume also that we have a fixed energy threshold value θ and a non-empty set $S \subset C$ of seeds indicating our OOI. Let $\mathcal{P}(S, \theta)$ be a family of all objects $P \subset C$, associated with $\boldsymbol{e}$, S, and θ, such that $\boldsymbol{e}(P) \leq \theta$, $S \subset P$, and every $c \in P$ is connected in P to some seed $s \in S$. Threshold θ will be always chosen so that the family $\mathcal{P}(S, \theta)$ is non-empty. Any of the region-based algorithms we consider here will return, as a delineated object, a set $P(S, \theta) \in \mathcal{P}(S, \theta)$. Usually (but not always) $P(S, \theta)$ is the smallest element of $\mathcal{P}(S, \theta)$.

In the case of any of the four methods FC, GC, WS, and LS, the value $\boldsymbol{e}(P)$ of the energy function is defined in terms of the boundary $\mathrm{bd}(P)$ of P, that is, the set $K = \mathrm{bd}(P)$ of all edges $\langle c, d\rangle$ of a graph $\boldsymbol{C} = \langle C, E\rangle$ with $c \in P$ and d not in P. We often refer to this boundary set K as a graph cut, since removing these edges from $\boldsymbol{C}$ disconnects P from its complement $C \setminus P$. The actual definition of $\boldsymbol{e}$ depends on the particular segmentation method.

Let $\kappa\colon E \to \mathbb{R}$ be a local cost function. For $\langle c, d\rangle \in E$ the value $\kappa(c, d)$ depends on the value of the image intensity function f on c, d, and (sometimes) nearby spels. Usually, the bigger is the difference between the values of $f(c)$ and $f(d)$, the smaller is the cost value $\kappa(c, d)$. This agrees with the intuition that the bigger the magnitude of the difference $f(c) - f(d)$ is, the greater is the chance that the "real" boundary of the object we seek is between these spels. In the FC algorithms, κ is called the affinity function. In the GC algorithms κ is treated as a weight function of the edges and is referred to as local cost function. For the classical GC algorithms, the energy function $\boldsymbol{e}(P)$ is defined as the sum of the weights of all edges in $K = \mathrm{bd}(P)$, that is, as $\sum_{\langle c,d\rangle \in K} \kappa(c, d)$. The delineations for the FC family of algorithms are obtained with the energy function $\boldsymbol{e}(P)$ defined as the maximum of the weights of all edges in $K = \mathrm{bd}(P)$, that is, as $\max_{\langle c,d\rangle \in K} \kappa(c, d)$. The same maximum function works also for the WS family with an appropriately chosen κ. The energy function for LS is more complicated, as it depends also on the geometry of the boundary, specifically its curvature.

11.2 Threshold-Indicated Fuzzy Connected Objects

Let $I = \langle \boldsymbol{C}, f\rangle$ be a digital image, with the scene $\boldsymbol{C} = \langle C, E\rangle$ being identified with a graph. As indicated above, the FC segmentations require a local measure of connectivity κ associated with I, known as affinity function, where for a graph edge $\langle c, d\rangle \in E$ (i.e., for adjacent c and d) the number $\kappa(c, d)$ (edge weight) represents a measure of how strongly spels c and d are connected to each other in a local sense. The most prominent affinities used so far are as follows [26], where $\sigma > 0$ is a fixed constant. The homogeneity-based affinity

$$\psi_\sigma(c, d) = e^{-||f(c)-f(d)||^2/\sigma^2} \quad \text{where} \quad \langle c, d\rangle \in E \tag{11.1}$$

with its value being close to 1 (meaning that c and d are well connected) when the spels have very similar intensity values; ψ_σ is related to the notion of directional derivative.

The object feature-based affinity (single object case, with an expected intensity vector $m \in \mathbb{R}^k$ for the object)

$$\phi_\sigma(c,d) = e^{-\max\{||f(c)-m||,||f(d)-m||\}^2/\sigma^2} \quad \text{where} \quad \langle c,d\rangle \in E \tag{11.2}$$

with its value being close to one when both adjacent spels have intensity values close to m. The weighted averages of these two forms of affinity functions – either additive or multiplicative – have also been used. The values of these affinity functions, used in the presented algorithms, are in the interval $[0,1]$.

11.2.1 Absolute Fuzzy Connectedness Objects

Let κ be an affinity associated with a digital image I. As stated in Section 11.1, an FC delineated object $P_{\max}(S,\theta)$, indicated by a set S of seeds and an appropriate threshold θ, can be defined as

$$P_{\max}(S,\theta) \text{ is the smallest set belonging to the family } \mathcal{P}_{FC}(S,\theta), \tag{11.3}$$

where $\mathcal{P}_{FC}(S,\theta)$ is the family of all sets $P \subset C$ such that: (i) $S \subset P$; (ii) every $c \in P$ is connected in P to some $s \in S$; (iii) $\kappa(c,d) \le \theta$ for all boundary edges $\langle c,d\rangle$ of P (i.e., $\boldsymbol{e}(P) = \max_{\langle c,d\rangle \in \mathrm{bd}(P)} \kappa(c,d) \le \theta$). This definition of the object is very convenient for the comparison of FC with GC and with the other two methods. Nevertheless, for the actual implementation of the FC algorithm, it is more convenient to use another definition, standard in the FC literature. The equivalence of both approaches is given by Theorem 1.

A path strength of a path $p = \langle c_1,\ldots,c_k\rangle$, $k > 1$, is defined as $\mu(p) \stackrel{\text{def}}{=} \min\{\kappa(c_{i-1},c_i)\colon 1 < i \le k\}$, that is, the strength of the κ-weakest link of p. For $k = 1$ (i.e., when p has length 1) we associate with p the strongest possible value: $\mu(p) \stackrel{\text{def}}{=} 1$.[4] For $c,d \in A \subseteq C$, the (global) *κ-connectedness strength in A between c and d* is defined as the strength of a strongest path in A between c and d; that is,

$$\mu^A(c,d) \stackrel{\text{def}}{=} \max\left\{\mu(p)\colon p \in \mathbb{P}^A_{cd}\right\}. \tag{11.4}$$

Notice that $\mu^A(c,c) = \mu(\langle c\rangle) = 1$. We will often refer to the function μ^A as a connectivity measure (on A) induced by κ. For $c \in A \subseteq C$ and a non-empty $D \subset A$, we also define $\mu^A(c,D) \stackrel{\text{def}}{=} \max_{d\in D} \mu^A(c,d)$. The standard definition of an FC delineated object, indicated by a set S of seeds and an appropriate

[4] For $k = 1$ the set $\{\kappa(c_{i-1},c_i)\colon 1 < i \le k\}$ is empty, so the first part of the definition leads to equation $\mu(\langle c_1\rangle) = \min\emptyset$. This agrees with our definition of $\mu(\langle c_1\rangle) = 1$ if we define $\min\emptyset$ as equal to 1, the highest possible value for κ. Thus, we will assume that $\min\emptyset = 1$.

threshold $\theta < 1$ and referred to as Absolute Fuzzy Connectedness (AFC) object, is given as $P_{S\theta} = \{c \in C\colon \theta < \mu^C(c, S)\}$.[5]

Theorem 1. *$P_{S\theta} = P_{\max}(S, \theta)$ for all $S \subset C$ and $\theta < 1$.*

11.2.2 Robustness of Objects

If a set of seeds S contains only one seed s, then we will write $P_{s\theta}$ for the object $P_{S\theta} = P_{\{s\}\theta}$. It is easy to see that $P_{S\theta}$ is a union of all objects $P_{s\theta}$ for $s \in S$, that is, $P_{S\theta} = \bigcup_{s\in S} P_{s\theta}$. Actually, if $G_\theta = \langle C, E_\theta\rangle$ is a graph with E_θ consisting of the scene graph edges $\langle c, d\rangle$ with weight $\kappa(c, d)$ greater than θ, then $P_{s\theta}$ is a connected component of G_θ containing s, and $P_{S\theta}$ is a union of all components of G_θ intersecting S.

One of the most important properties of the AFC objects is known as robustness. Intuitively, this property states that the FC delineation results do not change if the seeds S indicating an object are replaced by another nearby set T of seeds. Formally, it reads as follows.

Theorem 2. (Robustness) *For every digital image I on a scene $\boldsymbol{C} = \langle C, E\rangle$, every $s \in C$ and $\theta < 1$, if $P_{s\theta}$ is an associated FC object, then $P_{T\theta} = P_{s\theta}$ for every non-empty $T \subset P_{s\theta}$. More generally, if $S \subset C$ and $T \subset P_{S\theta}$ intersects every connected component of G_θ intersecting $P_{S\theta}$ (i.e., $T \cap P_{s\theta} \neq \emptyset$ for every $s \in S$), then $P_{T\theta} = P_{S\theta}$.*

The proof of this result follows easily from our graph interpretation of the object, as indicated above. The proof based only on the topological description of the scene can be found in [2, 5]. The robustness property constitutes the strongest argument for defining the objects in the FC fashion. Note, that none of the other algorithms discussed here have this property.

11.2.3 Algorithm for Delineating Objects

The algorithm presented below comes from [1].

Algorithm $\kappa\theta FOEMS$
Input: Scene $\boldsymbol{C} = \langle C, E\rangle$, affinity κ defined on an image $I = \langle \boldsymbol{C}, f\rangle$, a set $S \subset C$ of seeds indicating the object and a threshold $\theta < 1$.
Output: AFC object $P_{S\theta}$ for the image I.
Auxiliary Data Structures: A characteristic function $g\colon C \to \{0, 1\}$ of $P_{S\theta}$ and a queue Q of spels.

[5] In the literature an AFC object is usually arrived at (see [3, 5]) as $P^{\leq}_{S\theta} = \{c \in C\colon \theta \leq \mu^C(c, S)\}$. However, if θ^+ denotes the smallest number greater than θ of the form $\kappa(c, d)$, with $\langle c, d\rangle \in E$, then $P_{S\theta} = P^{\leq}_{S\theta^+}$. Thus, our definition of AFC object can be also expressed in the standard form, with just slightly different threshold. On the other hand, the following presentation is considerably easier expressible with the AFC object defined with the strict inequality.

begin

1. set $g(s) = 1$ for all $s \in S$ and $g(c) = 0$ for all $c \in C \setminus S$;
2. push to Q all spels $c \in C$ for which $\kappa(c, s) > \theta$ for some $s \in S$;
3. *while* Q is not empty *do*
4. remove a spel c from Q;
5. *if* $g(c) = 0$ *then*
6. set $g(c) = 1$;
7. push to Q all spels $d \in C$ for which $\kappa(d, c) > \theta$;
8. *endif*;
9. *endwhile*;
10. create $P_{S\theta}$ as a set of all spels c with $g(c) = 1$;

end

It is easy to see that $\kappa\theta FOEMS$ runs in linear time with respect to the size n of the scene C. This is the case, since any spel can be pushed into the queue Q (Line 7) at most Δ-many times, where Δ is the degree of the graph $\boldsymbol{C}$ (i.e., the largest number of spels that can be adjacent to a single spel; e.g., $\Delta = 26$ for the 26-adjacency). Specifically, $\kappa\theta FOEMS$ runs in time of order $O(\Delta n)$.

11.3 Optimization in Foreground-Background Case

So far, we discussed algorithms delineating an object, P, indicated by some seeds S belonging to P. Since we had no direct information on the spatial extent of the desired object, the actual extent of the delineated object P was regulated only by a mysterious parameter: a threshold θ setting the upper limit on the energy function value $\boldsymbol{e}(P)$. The difficulty of choosing this threshold is overcome by setting up and solving an appropriate optimization problem for an energy function $\boldsymbol{e}$. The setting part is done as follows.

First, we choose a proper initial condition, which, in the case of FC and GC algorithms, consists of indicating not only the foreground object (i.e., the OOI) by a set S of seeds, but also a background (i.e., everything except the OOI) by another set T of seeds. The stipulation is that S is contained in the delineated P, while T is disjoint with P. This ensures that we will consider only non-trivial sets P as possible choices for the object.

Let $\mathcal{P}(S, T)$ be the family of all sets $P \subset C$ such that $S \subset P$ and $T \cap P = \emptyset$. We like the desired object P to minimize the energy $\boldsymbol{e}(P)$ over all $P \in \mathcal{P}(S, T)$, that is, sets P satisfying the initial condition indicated by seeds S and T. In other words, if we define $\boldsymbol{e}_{\min} = \min\{\boldsymbol{e}(P)\colon P \in \mathcal{P}(S, T)\}$, then the OOI $P_{S,T}$ will be chosen, by an algorithm, as an element of the family $\mathcal{P}_{\min} = \{P \in \mathcal{P}(S, T)\colon \boldsymbol{e}(P) = \boldsymbol{e}_{\min}\}$. This is a typical setup for the energy optimization image delineation algorithms.

Notice that, although the minimal energy $\boldsymbol{e}_{\min}$ is always uniquely defined, the family $\mathcal{P}_{\min}$ may have more than one element, so our solution $P_{S,T} \in \mathcal{P}_{\min}$ still may not be uniquely determined. In the case of GC framework, the family

$\mathcal{P}_{\min}$ has always the smallest element (smallest in terms of inclusion) and this element is taken as $P_{S,T}$. The situation is the same in the FC framework, when S is a singleton. In the case when S has more seeds, the family $\mathcal{P}_{\min}$ is refined to a smaller family $\mathcal{P}^*_{\min}$ and $P_{S,T}$ is the smallest element of $\mathcal{P}^*_{\min}$. All of this is discussed in more detail below.

11.3.1 Relative Fuzzy Connectedness

In the fuzzy connectedness framework, the optimization technique indicated above is called Relative Fuzzy Connectedness (RFC). Once again, the actual definition of the RFC object $P_{S,T}$ (see [2]) is in a slightly different format from the one indicated above – it emphasizes the competition of seed sets S and T for attracting a given spel c to their realms. The attraction is expressed in terms of the strength of global connectedness $\mu^C(c,S)$ and $\mu^C(c,T)$: $P_{S,T}$ claims a spel c when $\mu^C(c,S)$ exceeds $\mu^C(c,T)$, that is,

$$P_{S,T} = \{c \in C\colon \mu^C(c,S) > \mu^C(c,T)\}$$

Notice that, $P_{S,T} = \{c \in C\colon (\exists s \in S)\mu^C(c,s) > \mu^C(c,T)\} = \bigcup_{s\in S} P_{\{s\},T}$, as $\mu^c(c,S) = \max_{s\in S}\mu^C(c,s)$. Below, we will show that, if the number $\mu^C(S,T) = \max_{s\in S}\mu^C(s,T)$ is less than 1, then $P_{S,T} \in \mathcal{P}(S,T)$, that is, that $P_{S,T}$ contains S and is disjoint with T. (If $\mu^C(S,T) = 1$, then sets S and T need not be disjoint. In this case the set $P_{S,T}$ is empty.) It is also important that

$$\text{if } P \in \mathcal{P}(S,T), \text{ then } \boldsymbol{e}(P) \geq \mu^C(S,T) \tag{11.5}$$

Indeed, choose a path $p = \langle c_1, \ldots, c_k\rangle$ from $s \in S$ to a $t \in T$ such that $\mu(p) = \mu^C(S,T)$. Since $c_1 = s \in P$ and $c_k = t \notin P$, there exists a $j \in \{2,\ldots,k\}$ with $c_{j-1} \in P$ while $c_j \notin P$. This means that $\langle c_{j-1}, c_j\rangle \in \mathrm{bd}(P)$. Hence, $\boldsymbol{e}(P) = \max_{\langle c,d\rangle\in \mathrm{bd}(P)}\kappa(c,d) \geq \kappa(c_{j-1},c_j) \geq \min\{\kappa(c_{i-1},c_i)\colon 1 < i \leq k\} = \mu(p) = \mu^C(S,T)$.

Next note that each object $P_{\{s\},T}$ is indeed a result of the optimization, as stated above.

Lemma 1. *Assume that $\theta_s = \mu^C(s,T) < 1$. Then $P_{\{s\},T} = P_{s\theta_s}$. Moreover, θ_s equals $\boldsymbol{e}_{\min} = \min\{\boldsymbol{e}(P)\colon P \in \mathcal{P}(\{s\},T)\}$ and $P_{s\theta_s}$ is the smallest set in the family $\mathcal{P}_{\min} = \{P \in \mathcal{P}(\{s\},T)\colon \boldsymbol{e}(P) = \boldsymbol{e}_{\min}\}$.*

The description of the RFC object $P_{S,T}$ when S has more than one seed is given in the following theorem. Intuitively, it says that each seed $s \in S$ generates separately its own part $P_{\{s\},T} \in \mathcal{P}(\{s\},T)$ and although their union, $P_{S,T}$, minimizes only its own lower bound $\theta_S = \mu^C(S,T)$, each component $P_{\{s\},T}$ minimizes its own version of the minimum, $\theta_s = \mu^C(s,T)$, which may be (and often is) smaller than the global minimizer $\theta_S = \mu^C(S,T)$. In other words, the object $P_{S,T}$ can be viewed as a result of minimization procedure used separately for each $s \in S$, which gives a sharper result than a simple minimization of global energy for the entire object $P_{S,T}$.

Theorem 3. *Assume that* $\theta_S = \mu^C(S,T) < 1$. *Then* $\boldsymbol{e}(P_{S,T}) = \theta_S = \boldsymbol{e}_{\min}$ *and* $P_{S,T} = \bigcup_{s\in S} P_{s\theta_s}$ *is the smallest set in the family* $\mathcal{P}^*_{\min}$ *of the sets of the form* $\bigcup_{s\in S} P^s$, *where each* P^s *belongs to* $\mathcal{P}^s_{\min} = \{P \in \mathcal{P}(\{s\},T)\colon \boldsymbol{e}(P) = \theta_s\}$. *Moreover,* $\mathcal{P}^*_{\min} \subset \mathcal{P}_{\min}$.

11.3.2 Algorithm for Delineating Objects

The algorithm presented below is a multiseed version of the algorithm from [1]. It is a main step for defining the RFC object $P_{S,T}$.

Algorithm $\kappa FOEMS$

Input: Scene $\boldsymbol{C} = \langle C, E\rangle$, affinity κ defined on an image $I = \langle \boldsymbol{C}, f\rangle$, a set $T \subset C$.

Output: A connectivity function $h\colon C \to [0,1]$, $h(c) = \mu^C(c,T)$.

Auxiliary Data Structures: A queue Q of spels.

begin

1. set $h(t) = 1$ for all $t \in T$ and $h(c) = 0$ for all $c \in C \setminus T$;
2. push to Q all spels $c \in C$ for which $\kappa(c,t) > 0$ for some $t \in T$;
3. *while* Q is not empty *do*
4. remove a spel c from Q;
5. find $M = \max\{\min\{h(d), \kappa(d,c)\}\colon \langle d,c\rangle \in E\}$
6. *if* $M > h(c)$ *then*
7. set $h(c) = M$;
8. push to Q all $d \in C$ for which $\min\{M, \kappa(c,d)\} > h(d)$;
9. *endif*;
10. *endwhile*;
11. output connectivity function $h\colon C \to [0,1]$, $h(c) = \mu^C(c,T)$;

end

The algorithm runs in quadratic time with respect to the size n of a scene $\boldsymbol{C}$. More precisely, the maximal number of possible values for the connectivity function h is the size of the range of κ, which does not exceed the size of the set of all edges E, that is, Δn. Therefore, each spel d may be pushed back to Q at most Δn^2 many times: when the value $h(c)$ is changed (maximum Δn-many times) for each of Δ-many spels c adjacent to d. Since each instance of performing the *while* command operation is of time order $O(\Delta)$, the $\kappa FOEMS$ ends, in the worst case, in time of order $O(\Delta^2 n^2)$.

If a connectivity function $h(c) = \mu^C(c,T)$ is calculated, then numbers $\theta_s = \mu^C(s,T) < 1$ are readily available, and object $P_{S,T} = \bigcup_{s\in S} P_{s\theta_s}$ can be delineated, in quadratic time of order $O(\Delta^2 n^2)$, by calling algorithm $\kappa\theta FOEMS$ for each $s \in S$.

11.3.3 Graph Cut Delineation

For the GC algorithms, a graph $G^I = \langle V, E\rangle$ associated with the image $I = \langle \boldsymbol{C}, f\rangle$, where $\boldsymbol{C} = \langle C, \alpha\rangle$, is a slight modification of the graph $\langle C, \alpha\rangle$ discussed

above. Specifically, the set of vertices V is defined as $C \cup \{s,t\}$, that is, the standard set C of image vertices is expanded by two new additional vertices s and t called terminals. Individually, s is referred to as source and t as sink. The set of edges is defined as $E = \alpha \cup \{\langle b,d\rangle\colon$ one of b,d is in C, the other in $\{s,t\}\}$. In other words, the edges between vertices in C remains as in $\boldsymbol{C}$, while we connect each terminal vertex to each $c \in C$.

The simplest way to think about the terminals is that they serve as the seed indicators: s for seeds $S \subset C$ indicating the object; t for seeds $T \subset C$ indicating the background. The indication works as follows. For each edge connecting a terminal $r \in \{s,t\}$ with a $c \in C$ associate the weight: ∞ if either $r = s$ and $c \in S$, or $r = t$ and $c \in T$; and 0 otherwise. This means, that the source s has infinitely strong connection to any seed c in S, and the weakest possible to any other spel $c \in C$. (We assume that all weights are nonnegative, that is, in $[0,\infty]$.) Similarly, for the sink t and seeds c from T.

Now, assume that for every edge $\langle c,d\rangle \in \alpha$ we give a weight $\kappa(c,d)$ associated with the image $I = \langle \boldsymbol{C}, f\rangle$. Since the algorithm for delineating RFC object uses only the information on the associated graph (which includes the weights given by the affinity κ), we can delineate RFC object $P^*_{\{s\},\{t\}} \subset V$ associated with this graph G^I. It is easy to see that the RFC object $P_{S,T} \subset C$ associated with I is equal to $P^*_{\{s\},\{t\}} \cap C$. Similarly, for $\theta < 1$, if $P^*_{s\theta} \subset V$ is an AFC object associated with the graph G^I, then the AFC object $P_{S\theta} \subset C$ associated with I is equal to $P^*_{S\theta} \cap C$. All of this proves that, from the FC framework point of view, replacing the graph $G = \langle C, \alpha\rangle$ with G^I is only technical in nature and results in no delineation differences.

Historically, the rationale for using in GC frameworks graphs G^I, with distinctive terminals, is algorithmic in nature. More precisely, for a weighted graph $G = \langle V,E\rangle$ with positive weights and two distinct vertices s and t indicated in it, there is an algorithm returning the smallest set P_G in the family $\mathcal{P}_{\min} = \{P \in \mathcal{P}(s,t)\colon \boldsymbol{e}(P) = \boldsymbol{e}_{\min}\}$, where $\mathcal{P}(s,t) = \{P \subset V \setminus \{t\}\colon s \in P\}$, $\boldsymbol{e}_{\min} = \min\{\boldsymbol{e}_\Sigma(P)\colon P \in \mathcal{P}(s,t)\}$, $\boldsymbol{e}_\Sigma(P) = \sum_{e \in \mathrm{bd}(P)} w_e$, and w_e is the weight of the edge e in the graph.

Now, let $G^I = \langle C \cup \{s,t\}\rangle, E\rangle$ be the graph associated with an image I as described above, that is, weights of edges between spels from C are obtained from the image I (in a manner similar to the affinity numbers) and weights between the other edges by seed sets S and T indicating foreground and background. It is easy to see that the object $P^\Sigma_{S,T} = C \cap P_{G^I}$ contains S, is disjoint with T, and has the smallest cost $\boldsymbol{e}_\Sigma$ among all such sets. Thus, the format of definition of the GC object $P^\Sigma_{S,T}$ is the same as that for RFC object $P_{S,T}$, the difference being only the energy functions $\boldsymbol{e}$ they use.

In spite of similarities between the GC and RFC methodologies as indicated above, there are also considerable differences between them. There are several theoretical advantages of the RFC framework over GC in this setting.

- *Speed:* The FC algorithms run faster than those for GC. Theoretical estimation of FC algorithms worst scenario run time (for slower RFC) is

$O(n^2)$ with respect to the scene size n (Sect. 11.3.2), while the best theoretical estimation of the run time for delineating $P^{\Sigma}_{S,T}$ is of order $O(n^3)$ (for the best known algorithms) or $O(n^{2.5})$ (for the fastest currently known), see [15]. This is also confirmed by experimental comparisons.

- *Robustness:* The outcome of FC algorithms is unaffected by small (within the objects) changes of the position of seeds (Theorems 2 and 4). On the other hand, the results of GC delineation may become sensitive for even small perturbations of the seeds.
- *Multiple objects:* The RFC framework handles easily the segmentation of multiple objects, retaining its running time estimate and robustness property (Sect. 11.4.1). The GC in the multiple object setting leads to an NP-hard problem [12], so all existing algorithms for performing the required precise delineation run in exponential time. However, there are algorithms that render approximate solutions for such GC problems in a practical time [12].
- *Shrinking problem:* In contrast to RFC methods, the GC algorithms have a tendency of choosing the objects with very small size of the boundary, even if the weights of the boundary edges is very high [16, 19]. This may easily lead to the segmented object being very close to either the foreground seed set S, or the complement of the background seed set T. Therefore, the object returned by GC may be far from desirable. This problem has been addressed by many authors, via modification of the GC method. Notice that RFC methods do not have any shrinking problem.
- *Iterative approach:* The FC framework allows an iterative refinement of its connectivity measure μ^A, which in turn makes it possible to redefine $\boldsymbol{e}$ as we go along. From the viewpoint of algorithm, this is a powerful strategy. No such methods exist for GC at present.

All of this said, it should be noticed that GC has also some nice properties that FC does not possess. First notice that the shrinking problem is the result of favoring shorter boundaries over the longer, that is, has a smoothing effect on the boundaries. This, in many (but not all) cases of medically important image delineations, is a desirable feature. There is no boundary smoothing factor built in to the FC basic framework and, if desirable, boundary smoothing must be done at the FC post processing stage.

Another nice feature of GC graph representation G^I of an image I is that the weights of edges to terminal vertices naturally represent the object feature-based affinity, see (11.2), while the weights of the edges with both vertices in C are naturally connected with the homogeneity type of affinity (11.1). This is the case, since homogeneity-based affinity (a derivative concept) is a binary relation in nature, while the object feature-based affinity is actually a unary relation. Such a clear cut distinction is difficult to achieve in FC framework, since it requires only one affinity relation in its setting.

11.4 Segmentation of Multiple Objects

Now, assume that we like to recognize $m > 1$ separate objects, $P_1, \ldots, P_m$, in the image $I = \langle \boldsymbol{C}, f \rangle$. What general properties the family $\mathcal{P} = \{P_1, \ldots, P_m\}$ should have? The term "segmentation" suggests that $\mathcal{P}$ should be a partition of a scene C, that is, that sets are *pairwise disjoint* (i.e., no two of then have common element) and that they *cover* C (i.e., $C = \bigcup_{i=1}^{m} P_i$). Unfortunately, insuring both of these properties is usually neither desirable not possible for the medical image segmentation problems. We believe, that the most reasonable compromise here is to assume that the objects P_i are pairwise disjoint, while they do not necessarily cover the entire image scene C. The motivation here is the delineation of major body organs (e.g., stomach, liver, pancreas, kidneys). Therefore, the term image segmentation refers to a family $\mathcal{P} = \{P_1, \ldots, P_m\}$ of pairwise disjoint objects for which the background set $B_{\mathcal{P}} = C \setminus \bigcup_{i=1}^{m} P_i$ might be nonempty.

It should be stressed, however, that some authors allow overlap of the objects, while ensuring that there is no nonempty background $B_{\mathcal{P}}$ [7,8]. Other methods (like classical WS algorithms) return a partition of a scene.

11.4.1 Relative Fuzzy Connectedness

Assume that for an image $I = \langle \boldsymbol{C}, f \rangle$ we have a pairwise disjoint family $\mathcal{S} = \{S_1, \ldots, S_m\}$ of sets of seeds, each S_i indicating an associated object P_i. If for each i we put $T_i = \left(\bigcup_{j=1}^{m} S_j\right) \setminus S_i$, then the RFC segmentation is defined as a family $\mathcal{P} = \{P_{S_i\mathcal{S}} \colon i = 1, \ldots, m\}$, where each object $P_{S_i\mathcal{S}}$ is equal to $P_{S_i,T_i} = \{c \in C \colon \mu^C(c, S_i) > \mu^C(c, T_i)\}$.

Since, by Lemma 1, each P_{S_i,T_i} equals $\bigcup_{s\in S_i} P_{\{s\},T_i} = \bigcup_{s\in S} P_{s\theta_s}$, where $\theta_s = \mu^C(s, T_i)$, using the algorithms from Section 11.3.2, the partition $\mathcal{P}$ can be found in $O(n^2)$ time. Also, the robustness Theorem 2 can be modified to this setting as follows.

Theorem 4. (Robustness for RFC) *Let $\mathcal{S} = \{S_1, \ldots, S_m\}$ be a family of seeds in a digital image I and let $\mathcal{P} = \{P_{S_i\mathcal{S}} \colon i = 1, \ldots, m\}$ be an associated RFC segmentation. For every i and $s \in S_i$ let $g(s)$ be in $P_{\{s\},T_i}$. If $\mathcal{S}' = \{S'_1, \ldots, S'_m\}$, where each $S'_i = \{g(s) \colon s \in S_i\}$, then $P_{S_i\mathcal{S}} = P_{S'_i\mathcal{S}'}$ for every i.*

In other words, if each seed s present in $\mathcal{S}$ is only "slightly" shifted to a new position $g(s)$, then the resulting RFC segmentation $\{P_{S'_i\mathcal{S}'} \colon i = 1, \ldots, m\}$ is identical to the original one $\mathcal{P}$.

When an RFC object $P_{S_i\mathcal{S}}$ is indicated by a single seed, then, by Theorem 3, it is equal to the AFC object $P_{s_i\theta_i}$ for appropriate threshold θ_i. But even when all objects are in such forms, different threshold θ_i need not be equal, each being individually tailored.

This idea is best depicted schematically (Fig. 11.1). Figure 11.1(a) represents a schematic scene with a uniform background and four distinct areas

denoted by S, T, U, W, and indicated by seeds marked by $\times$. It is assumed that each of these areas is uniform in intensity and the connectivity strength within each of these areas has the maximal value of 1, the connectivity between the background and any other spel is ≤ 0.2, while the connectivity between the adjacent regions is as indicated in the figure: $\mu(s,t) = 0.6$, $\mu(s,u) = 0.5$, and $\mu(u,w) = 0.6$. (Part b): The RFC segmentation of three objects indicated by seeds s, t, and u, respectively. (Part c):Three AFC objects indicated by the seeds s, t, u and delineated with threshold $\theta = 0.6$. Notice that while $P_{s,\{s,t,u\}} = P_{s,.6}$ and $P_{t,\{s,t,u\}} = P_{t,.6}$, object $P_{u,.6}$ is smaller than RFC indicated $P_{u,\{s,t,u\}}$. (Part d): Same as in Part (c) but with $\theta = 0.5$. Note that while $P_{u,\{s,t,u\}} = P_{u,.5}$, objects $P_{s,.5}$ and $P_{t,.5}$ coincide and lead to an object bigger than $P_{s,\{s,t,u\}}$ and $P_{t,\{s,t,u\}}$.

11.4.2 Iterative Relative Fuzzy Connectedness

The RFC segmentation $\mathcal{P} = \{P_{S_i\mathcal{S}} : i = 1, \ldots, m\}$ of a scene can still leave quite a sizable "leftover" background set $B = B_{\mathcal{P}}$ of all spels c outside any of the objects wherein the strengths of connectedness are equal with respect to the seeds. The goal of the Iterative Relative Fuzzy Connectedness (IRFC) is to find a way to naturally redistribute some of the spels from $B_{\mathcal{P}}$ among the object regions in a new generation (iteration) of segmentation. Another motivation for IRFC is to overcome the problem of "path strength dilution" within the same object, of paths that reach the peripheral subtle and thin aspects of the object.

In the left part of Figure 11.2, two object regions A and B, each with its core and peripheral subtle parts, are shown, a situation like the arteries and veins being juxtaposed. Owing to blur, partial volume effect and other shortcomings, the strongest paths from s_1 to t_1, s_1 to t_2, s_2 to t_1, and s_2 to t_2 are all likely to assume similar strengths. As a consequence, the spels in the dark areas may fall in $B_{\mathcal{P}}$, the unclaimed background set.

The idea of IRFC is to treat the RFC delineated objects $P_{S_i\mathcal{S}}$ as the first iteration $P^1_{S_i\mathcal{S}}$ approximation of the final segmentation, while the next step

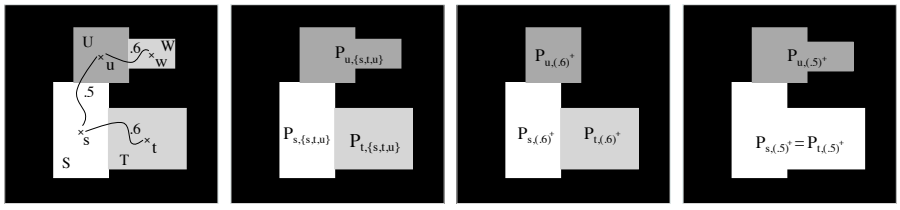

(a) schematic scene (b) segmentation (c) $\theta = 0.6$ (d) $\theta = 0.5$

Fig. 11.1. Relative fuzzy connectedness. Each object is optimized separately. Panels (c) and (d) show delineations.

iteration is designed to redistribute some of the background spels $c \in B_{\mathcal{P}}$, for which $\mu^C(c, S_i) = \mu^C(c, T_i)$ for some i. Such a tie can be resolved if the strongest paths justifying $\mu^C(c, S_i)$ and $\mu^C(c, T_i)$ cannot pass through the spels already assigned to another object. In other words, we like to add spels from the set $P^* = \{c \in B\colon \mu^{B \cup P_{S_i\mathcal{S}}}(c, S_i) > \mu^{B \cup P_{S_j\mathcal{S}}}(c, S_j)$ for every $j \neq i\}$, to a new generation $P^2_{S_i\mathcal{S}}$ of $P^1_{S_i\mathcal{S}}$, that is, define $P^2_{S_i\mathcal{S}}$ as $P^1_{S_i\mathcal{S}} \cup P^*$. This formula can be taken as a definition. However, from the algorithmic point of view, it is more convenient to define $P^2_{S_i\mathcal{S}}$ as

$$P^2_{S_i\mathcal{S}} = P^1_{S_i\mathcal{S}} \cup \left\{c \in C \setminus P^1_{S_i\mathcal{S}}\colon \mu^C(c, S_i) > \mu^{C \setminus P^1_{S_i\mathcal{S}}}(c, T_i)\right\}$$

while the equation $P^2_{S_i\mathcal{S}} = P^1_{S_i\mathcal{S}} \cup P^*$ always holds, as proved in [5, thm. 3.7]. Thus, the IRFC object is defined as $P^\infty_{S_i\mathcal{S}} = \bigcup_{k=1}^\infty P^k_{S_i\mathcal{S}}$, where sets $P^k_{S_i\mathcal{S}}$ are defined recursively by the formulas $P^1_{S_i\mathcal{S}} = P_{S_i\mathcal{S}}$ and

$$P^{k+1}_{S_i\mathcal{S}} = P^k_{S_i\mathcal{S}} \cup \left\{c \in C \setminus P^k_{S_i\mathcal{S}}\colon \mu^C(c, S_i) > \mu^{C \setminus P^k_{S_i\mathcal{S}}}(c, T_i)\right\} \tag{11.6}$$

The right side of Figure 11.2 illustrates these ideas pictorially. The initial segmentation is defined by RFC conservatively, so that $P_{S_i\mathcal{S}}$ corresponds to the core aspects of the object identified by seed $s \in S_i$ (illustrated by the hatched area containing s). This leaves a large boundary set B where the strengths of connectedness with respect to the different seeds are equal (illustrated by the shaded area containing c). In the next iteration, the segmentation is improved incrementally by grabbing those spels of B that are connected more strongly to $P_{S_i\mathcal{S}}$ than to sets $P_{S_j\mathcal{S}}$. When considering the object associated with s, the "appropriate" path from s to any $c \in B$ is any path in C. However, all objects have to compete with the object associated with s by allowing paths from their respective seeds $t \in T_i$ to c not to go through $P_{S_i\mathcal{S}}$ since this set has already been declared to be part of the object of s.

The IRFC segmentation is robust in the sense of Theorem 4, where in its statement the objects $P_{S_i\mathcal{S}}$ are replaced by the first iteration $P^1_{S_i\mathcal{S}}$ of $P^\infty_{S_i\mathcal{S}}$.

Fig. 11.2. RFC vs. IRFC. Left: The strongest paths from s_1 to t_1, s_1 to t_2, s_2 to t_1, and s_2 to t_2 are likely to have the same strength because of partial volume effects; Right: Pictorial illustration of IRFC advantages over RFC.

This follows easily from Theorem 4 [5]. It is also worth to notice that the witnessing strongest paths from $c \in P^{\infty}_{S_i\mathcal{S}}$ to S_i can be found in $P^{\infty}_{S_i\mathcal{S}}$ [5].

11.4.3 Algorithm for Iterative Relative Fuzzy Connectedness

The algorithm presented below comes from [5]. Note that we start the recursion with $P^0_{S_i\mathcal{S}} = \emptyset$. It is easy to see that with such definition $P^1_{S_i\mathcal{S}}$ obtained with (11.6) is indeed equal to $P_{S_i\mathcal{S}}$.

Algorithm $\kappa IRMOFC$

Input: Scene $\boldsymbol{C} = \langle C, E\rangle$, affinity κ defined on an image $I = \langle \boldsymbol{C}, f\rangle$, a family $\mathcal{S} = \{S_1, \ldots, S_m\}$ of pairwise disjoint set of seeds, a sequence $\langle T_1, \ldots, T_m\rangle$, with $T_i = \left(\bigcup_{j=1}^{m} S_j\right) \setminus S_i$ for every i.

Output: A sequence $\langle P^{\infty}_{S_1\mathcal{S}}, \ldots, P^{\infty}_{S_m\mathcal{S}}\rangle$ forming IRFC segmentation.

Auxiliary Data Structures: A sequence of characteristic functions $g_i \colon C \to \{0,1\}$ of objects $P^k_{S_i\mathcal{S}}$ and affinity κ_{g_i} equal to κ for pairs $\langle c, d\rangle$ with $g_i(c) = g_i(d) = 0$, and 0 otherwise. Note that $\mu^C(\cdot, T_i)$ for κ_{g_i} equals to $\mu^{C\setminus P_{S_i\mathcal{S}}}(\cdot, T_i)$ for $P_{S_i\mathcal{S}}$ indicated by g_i.

begin

1. *for* $i = 1$ *to* m *do*
2. invoke $\kappa FOEMS$ to find $h_0(\cdot) = \mu^C(\cdot, S_i)$;
3. initiate $g_i(c) = 0$ for all $c \in C$;
4. set $\kappa_{g_i} = \kappa$ and $flag =$ true;
5. *while* $flag =$ true *do*;
6. set $flag =$ false;
7. invoke $\kappa FOEMS$ to find $h(\cdot) = \mu^C(\cdot, T_i)$ for κ_{g_i};
8. *for* all $c \in C$ *do*
9. *if* $g_i(c) = 0$ and $h_0(c) > h(c)$ *then*
10. set $g_i(c) = 1$ and $flag =$ true;
11. *for* every $d \in C$, $d \neq c$, adjacent to c *do*
12. set $\kappa_{g_i}(c, d) = 0$ and $\kappa_{g_i}(d, c) = 0$;
13. *endfor*;
14. *endif*;
15. *endfor*;
16. *endwhile*;
17. *endfor*;
18. output sets $P^{\infty}_{S_i\mathcal{S}}$ indicated by characteristic functions g_i;

end

The proof that the algorithm stops and returns proper objects can be found in [5]. Since it can enter while loop at most once for each updated spel, it enters it $O(n)$ times, where n is the size of C. Since $\kappa FOEMS$ runs in time of order $O(\Delta^2 n^2)$, the worst scenario for $\kappa IRMOFC$ is that it runs in time of order $O(\Delta^2 n^3)$.

A slightly different approach to calculating IRFC objects comes from the Image Foresting Transform (IFT) [20,27]. This approach distributes the spels

unassigned by IRFC to different objects, according to some ad hoc algorithmic procedure.

11.4.4 Variants of IRFC

In the papers [7–9] (in particular, see [8, page 465]), the authors employ different affinity κ_i for each i-th object to be delineated, and apply the algorithm that returns the objects $\hat{P}^{\infty}_{S_i\mathcal{S}} = \bigcup_{k=0}^{\infty} \hat{P}^k_{S_i\mathcal{S}}$, with sets $\hat{P}^k_{S_i\mathcal{S}}$ being defined recursively by the formulas $\hat{P}^0_{S_i\mathcal{S}} = \emptyset$ and

$$\hat{P}^{k+1}_{S_i\mathcal{S}} = \hat{P}^k_{S_i\mathcal{S}} \cup \bigcup_{j\neq i} \left\{ c \in C \setminus \hat{P}^k_{S_i\mathcal{S}} \colon \mu_i^C(c, S_i) \geq \mu_j^{C\setminus \hat{P}^k_{S_i\mathcal{S}}}(c, S_j) \right\} \tag{11.7}$$

where μ_j is the global connectivity measure associated with the affinity κ_j.

In general, the segmentations defined with different affinities, in the format of (11.7) (even with just one step iteration, that is, in the RFC mode), are neither robust nor have path connectedness property mentioned at the end of Section 11.4.2. (See [2].) Although, the lack of path connectedness property may seem to be of little consequence, it undermines the entire philosophy that stands behind IRFC definitions. Nevertheless, it solves some problems with dealing with the object-feature based affinity in single affinity mode, which was discussed in [28].

11.5 Scale-based and Vectorial Fuzzy Connectedness

In our discussion so far, when formulating affinities κ, we considered $\kappa(c, d)$ to depend only (besides the spatial relation of c and d) on the (vectorial or scalar) intensities $f(c)$ and $f(d)$ at c and d, cf. (11.1) and (11.2). This restriction can be relaxed, yielding us scale-based and vectorial affinity.

In scale-based FC [26], instead of considering just c and d, a "local scale region" around each of c and d is considered in scene C for defining κ. In the ball scale approach, this local region around c is the largest ball b_c, centered at c, which is such that the image intensities at spels within b_c are homogeneous. For defining $\kappa(c, d)$ then, the intensities within b_c and b_d are considered. Typically a filtered value $f'(x)$ is estimated for each $x \in \{c, d\}$ from all intensities within b_x by taking their weighted average, the weight determined by a k-variate Gaussian function centered at $f(x)$. The filtered values $f'(c)$ and $f'(d)$ are then used in defining $\kappa(c, d)$ instead of the original intensities $f(c)$ and $f(d)$. In place of the ball, an ellipsoid has also been proposed for the scale region, which leads to the tensor scale approach [29]. The underlying idea in these approaches is to reduce the sensitivity of FC algorithms to spel-level random noise. Note that when local scales are used in this manner, none of the theoretical constructs of FC needs change. Actually, the scale-based approach can be seen as a preprocessing step: replace the original intensity function f

with its scale-based filtered version f', and then proceed with the regular FC algorithm applied to the image $I' = \langle C, f' \rangle$ in place of $I = \langle C, f \rangle$.

In vectorial FC [6], the vectorial intensity function $f(x) \in \mathbb{R}^k$ is used in defining κ. For example, in such a case, (11.1) and (11.2) become k-variate Gaussian functions (i.e., we apply k-variate Gaussian to a vector, like $f(c) - f(d)$, instead of simple Gaussian function to its length $||f(c) - f(d)||$). Obviously, the scale concept can be combined with the vectorial idea [6]. In fact, these two concepts can be individually or jointly combined with the principles underlying AFC, RFC, and IRFC.

11.6 Affinity Functions in Fuzzy Connectedness

An affinity function for an image $I = \langle \boldsymbol{C}, f \rangle$, with $\boldsymbol{C} = \langle C, \alpha \rangle$, is a function, say κ, defined on a set $C \times C$. More precisely, it is of importance only for the adjacent pairs $\langle c, d \rangle$, that is, from $\alpha \subset C \times C$. The affinity functions defined in (11.1) and (11.2) have the values in the interval $[0, 1]$, are symmetric (i.e., $\kappa(c, d) = \kappa(d, c)$ for all $c, d \in C$) and have the property that $\kappa(c, c) = 1$ for all $c \in C$. We will refer to any such affinity as a standard affinity.

In general, any linearly ordered set $\langle L, \preceq \rangle$ can serve as a range (value set) of an affinity [30]: a function $\kappa \colon C \times C \to L$ is an affinity function (into $\langle L, \preceq \rangle$) provided κ is symmetric and $\kappa(a, b) \preceq \kappa(c, c)$ for every $a, b, c \in C$. Note that $\kappa(d, d) \preceq \kappa(c, c)$ for every $c, d \in C$. So, there exists an element in L, which we denote by a symbol $\mathbf{1}_\kappa$, such that $\kappa(c, c) = \mathbf{1}_\kappa$ for every $c \in C$. Notice that $\mathbf{1}_\kappa$ is the largest element of $L_\kappa = \{\kappa(a, b) \colon a, b \in C\}$, although it does not need to be the largest element of L. Clearly, any standard affinity κ is an affinity function with $\langle L, \preceq \rangle = \langle [0, 1], \leq \rangle$ and $\mathbf{1}_\kappa = 1$. In the discussion below, $\langle L, \preceq \rangle$ will be either the standard range $\langle [0, 1], \leq \rangle$ or $\langle [0, \infty], \geq \rangle$. Note that, in this second case, the order relation $\preceq$ is the *reversed* standard order relation $\geq$.

11.6.1 Equivalent Affinities

We say that the affinities $\kappa_1 \colon C \times C \to \langle L_1, \preceq_1 \rangle$ and $\kappa_2 \colon C \times C \to \langle L_2, \preceq_2 \rangle$ are *equivalent* (in the FC sense) provided, for every $a, b, c, d \in C$

$$\kappa_1(a, b) \preceq_1 \kappa_1(c, d) \quad \text{if and only if} \quad \kappa_2(a, b) \preceq_2 \kappa_2(c, d).$$

For example, it can be easily seen that for any constants $\sigma, \tau > 0$ the homogeneity-based affinities ψ_σ and ψ_τ, see (11.1), are equivalent, since for any pairs $\langle a, b \rangle$ and $\langle c, d \rangle$ of adjacent spels: $\psi_\sigma(a, b) < \psi_\sigma(c, d) \iff ||f(a) - f(b)|| > ||f(c) - f(d)|| \iff \psi_\tau(a, b) < \psi_\tau(c, d)$. (Symbol $\iff$ means "if and only if.") Equivalent affinities can be characterized as follows, where $\circ$ stands for the composition of functions, that is, $(g \circ \kappa_1)(a, b) = g(\kappa_1(a, b))$ [31].

Theorem 5. *Affinities $\kappa_1 \colon C \times C \to \langle L_1, \preceq_1 \rangle$ and $\kappa_2 \colon C \times C \to \langle L_2, \preceq_2 \rangle$ are equivalent if and only if there exists a strictly increasing function g from $\langle L_{\kappa_1}, \preceq_1 \rangle$ onto $\langle L_{\kappa_2}, \preceq_2 \rangle$ such that $\kappa_2 = g \circ \kappa_1$.*

The FC objects, defined in the previous sections, have the same definition with the general notion of affinity, when the standard inequality '$\leq$' is replaced by '$\preceq$.' The implications of and our interest in equivalent affinities are well encapsulated by the next theorem, which says that any FC segmentation (AFC, RFC, or IRFC) of a scene $\boldsymbol{C}$ remains unchanged if an affinity on C used to get the segmentation is replaced by an equivalent affinity.

Theorem 6. [31] *Let $\kappa_1 \colon C \times C \to \langle L_1, \preceq_1 \rangle$ and $\kappa_2 \colon C \times C \to \langle L_2, \preceq_2 \rangle$ be equivalent affinity functions and let $\mathcal{S}$ be a family of non-empty pairwise disjoint subsets of C. Then for every $\theta_1 \prec_1 \mathbf{1}_{\kappa_1}$ in L_1, there exists a $\theta_2 \prec_2 \mathbf{1}_{\kappa_2}$ in L_2 such that, for every $S \in \mathcal{S}$ and $i \in \{0, 1, 2, \ldots\}$, we have $P^{\kappa_1}_{S\theta_1} = P^{\kappa_2}_{S\theta_2}$, $P^{\kappa_1}_{S\mathcal{S}} = P^{\kappa_2}_{S\mathcal{S}}$, and $P^{i,\kappa_1}_{S\mathcal{S}} = P^{i,\kappa_2}_{S\mathcal{S}}$.*

Moreover, if $g \colon C \to C$ is a strictly monotone function such that $\kappa_2 = g \circ \kappa_1$ (which exists by Theorem 5), then we can take $\theta_2 = g(\theta_1)$.

Keeping this in mind, it makes sense to find for each affinity function an equivalent affinity in a nice form:

Theorem 7. [31] *Every affinity function is equivalent (in the FC sense) to a standard affinity.*

Once we agree that equivalent affinities lead to the same segmentations, we can restrict our attention to standard affinities without losing any generality of our method.

Next, we like to describe the natural FC equivalent representations of the homogeneity-based ψ_σ (11.1) and object feature-based ϕ_σ (11.2) affinities. The first of them, $\psi_\sigma(c, d)$, is equivalent to an approximation of the magnitude of the directional derivative $\left|D_{\overrightarrow{cd}} f(c)\right| = \left|\frac{f(c)-f(d)}{||c-d||}\right|$ of f in the direction of the vector $\overrightarrow{cd}$. If spels c and d are adjacent when $||c - d|| \leq 1$, then for adjacent $c, d \in C$ we have $\psi(c, d) \stackrel{\text{def}}{=} \left|D_{\overrightarrow{cd}} f(c)\right| = |f(c) - f(d)|$. Such defined ψ is an affinity with the range $\langle L, \preceq \rangle = \langle [0, \infty], \geq \rangle$. The equivalence of ψ with ψ_σ is justified by Theorem 5 and the Gaussian function $g_\sigma(x) = e^{-x^2/\sigma^2}$, as $\psi_\sigma(c, d) = (g_\sigma \circ \psi)(c, d)$ for any adjacent $c, d \in C$.

The natural form of the object feature-based ϕ_σ affinity (for one object) and a spel c is the number $||f(c) - m||$, a distance of the image intensity $f(c)$ at c from the expected object intensity m. For two adjacent distinct spels, this leads to the definition $\phi(c, d) = \max\{||f(c) - m||, ||f(d) - m||\}$. We also put $\phi(c, c) = 0$, to insure that ϕ is an affinity function, with the range $\langle L, \preceq \rangle = \langle [0, \infty], \geq \rangle$. Once again, ϕ is equivalent with ϕ_σ, as $\phi_\sigma = g_\sigma \circ \phi$.

The homogeneity-based connectivity measure, $\mu_\psi = \mu^C_\psi$, can be elegantly interpreted if the scene $\boldsymbol{C} = \langle C, f \rangle$ is considered as a topographical map in

which $f(c)$ represents an elevation at the location $c \in C$. Then, $\mu_\psi(c,d)$ is the highest possible step (a slope of f) that one must make in order to get from c to d with each step on a location (spel) from C and of unit length. In particular, the object $P^\psi_{s\theta} = \{c \in C \colon \theta > \mu_\psi(s,c)\}$ represents those spels $c \in C$ which can be reached from s with all steps lower than θ. Note that all we measure in this setting is the actual change of the altitude while making the step. Thus, this value can be small, even if the step is made on a very steep slope, as long as the path approximately follows the altitude contour lines – this is why on steep hills the roads zigzag, allowing for a small incline of the motion. On the other hand, the measure of the same step would be large, if measured with some form of gradient induced homogeneity-based affinity! (Compare Section 11.7.2.)

The object feature-based connectivity measure of one object has also a nice topographical map interpretation. For understanding this, consider a modified scene $\bar{\boldsymbol{C}} = \langle C, |f(\cdot) - m| \rangle$ (called membership scene in [1]) as a topographical map. Then the number $\mu_\phi(c,d)$ represents the lowest possible elevation (in $\bar{\boldsymbol{C}}$) which one must reach (a mountain pass) in order to get from c to d, where each step is on a location from C and is of unit length. Notice that $\mu_\phi(c,d)$ is precisely the degree of connectivity as defined by Rosenfeld [32–34]. By the above analysis, we brought Rosenfeld's connectivity also into the affinity framework introduced by [1], particularly as another object feature component of affinity.

11.6.2 Essential Parameters in Affinity Functions

Next, let us turn our attention to the determination of the number of parameters essential in defining the affinities:

- *Homogeneity-based affinity* ψ_σ has no essential parameter, that is, the parameter σ in its definition is redundant, as $\psi_\sigma = g_\sigma \circ \psi$ is equivalent to ψ, which is independent of σ. This beautiful characteristic says that FC partitioning of a scene utilizing homogeneity-based affinity is an inherent property of the scene and is independent of any parameters, besides a threshold in case of AFC.
- *Object feature-based affinity* ϕ_σ *for one object* has two explicit parameters, m and σ, of which only parameter m is essential. Parameter σ is redundant, since $\phi_\sigma = g_\sigma \circ \phi$ is equivalent to ϕ defined above.
- *Object feature-based affinity* $\bar{\phi}_{\bar{\sigma}}$ *for* $n > 1$ *objects* is usually defined as $\bar{\phi}(c,d) = \max_{i=1,\ldots,n} \phi_{\sigma_i}(c,d)$ [28], where each ϕ_{σ_i} is defined by (11.2), with the parameter m replaced with the ith object average intensity m_i. Here $\bar{\sigma} = \langle \sigma_1, \ldots, \sigma_n \rangle$. This affinity has $2n$ explicit parameters, but only $2n-1$ are essential. Indeed, if $\bar{\delta} = \langle 1, \delta_2, \ldots, \delta_n \rangle$, where $\delta_i = \sigma_i/\sigma_1$, then $\bar{\phi}_{\bar{\sigma}}$ and $\bar{\phi}_{\bar{\delta}}$ are equivalent, since $\bar{\phi}_{\bar{\delta}} = h_{\sigma_1} \circ \bar{\phi}_{\bar{\sigma}}$, where $h_\sigma(x) = x^{\sigma^2}$.

Similar results for the averages, additive and multiplicative, of ψ and ϕ, as well as their lexicographical order combination, can be found in [28].

11.7 Other Delineation Algorithms

We have already discussed deep similarities between FC and GC methods. In both cases, the image scene can be represented as weighted graphs (with different ways of assigning these weights) and the segmentations consist of different subsets P's of the graph vertices. In both cases, we associate with each object P in the graph its energy (cost) value $\boldsymbol{e}(P)$ represented in terms of the weights of edges in the boundary of P, that is, with one spel in P, another in its complement. The difference is the format of the energy cost function: in GC it is a sum of the weights of the boundary edges, while in FC it is the maximum among all these numbers.

11.7.1 Generalized Graph Cut

Despite the similarities, the segmentations resulting from FC and GC have different properties. For example, the FC segmentations are robust with respect to seed choice, but GC delineations are not. On the other hand, GC output smoothes the boundary of the resulting object (via penalizing long boundaries) – which is sometimes desirable – while FC have no such properties. An interesting problem was considered in [35]:

> "For what classes of graph energy cost functions $\boldsymbol{e}(P)$ (not necessarily defined in terms of the edge weights) can we find graph weights such that the GC optimization of the resulting graph is identical to the optimization of the original function $\boldsymbol{e}$?"

The necessary condition given there implies, in particular, that the maximum energy of FC cannot be represented that way. This also follows from the fact that FC and GC segmentations have different properties, like robustness.

It should be clear that, if one uses in FC an object feature-based affinity, then, under an interpretation of μ as Rosenfeld's degree of connectivity, the resulting segmented object is the water basin, as in the WS segmentations. If one desires more than one basin/object, then RFC results agree with the WS basin interpretation, as long as one "stops pumping the water" when a spill to another basin occurs.

At that point, we face a problem discussed in Section 11.4.1: should we leave the spels where competition breaks unassigned to any object, or should we find a way to redistribute them among the objects. In RFC we opt for the first of these choices. In standard WS, the second option is followed by "building the dams" at the "mountain passes" where conflict occurs, and then continuing "land submerging" process until every spel is assigned. In other words, the outcome of WS can be viewed as the outcome of RFC used with proper object feature-based affinity, if we opt for leaving unassigned the spels where "ties" occur.

In summary, the FC, GC, and WS methods, to which we will refer here as Generalized Graph (GG) methods, can be viewed as the same class of

segmentation methods, with their outcomes – resulting from the optimization of appropriate energy functions – obtained as segmentations of appropriate weighted graphs. This was clearly demonstrated above, if one chooses treating segmentation as an assignment of disjoint regions, when some spels belong to no object. In the other extreme, when the "spels with ties" are assigned according a proper (slightly ad hoc) procedures typical for each method, the GG algorithms are also equivalent. They all can be expressed in the IFT framework [20, 27, 36].

11.7.2 Level Set vs. Generalized Graph Cut

The relation of GG to LS is not straightforward. First of all, we will understand that the name relates to the image segmentation methods that have the following properties:

1. set the segmentation problem in the continuous setting (i.e., images are defined on the regions Ω in the Euclidean space $\mathbb{R}^{\mathfrak{n}}$, usually with $\mathfrak{n} = 2$ or $\mathfrak{n} = 3$), solve it as such, and, only at the last stage of method development, use discretization (i.e., finite approximation) of the continuous case to the the digital image case;
2. in the problem set-up, use an energy function $\boldsymbol{e}$ associating with image segmentation $\mathcal{P}$ its energy value $\boldsymbol{e}(\mathcal{P})$;
3. usually (but not always) considered as a problem solution a segmentation $\mathcal{P}$ that minimizes $\boldsymbol{e}$ in an appropriate class of segmentations;
4. usually (but not always) the minimization is achieved by variational methods, which leads to a differential equation and returns a local minimum for $\boldsymbol{e}$.

Some optimization methods, like active contour (snake) [37] satisfy all these properties, but are not region-based methods, since they concentrate on finding only parts of a region boundary at a time. Some others actually do not explicitly optimize an energy (i.e., there is no clear Step 3), but it can be viewed as a solution for a variational problem (i.e., Step 4), that is, a solution for an implicitly given optimization problem [24]. Perhaps the most influential and prominent LS delineation method is that of Mumford and Shah [38], and its special case, due to Chan and Vese [39].

The biggest difference between such described LS methods and GG methods is the property (1) of LS: it makes a precise theoretical comparison between the methods difficult, and, at the purely discrete level, actually impossible. This is the case, since the precise outcome of LS is a segmentation of Ω, while the other methods return segmentations on a discrete scene $\boldsymbol{C}$. If we try to compare LS and GG segmentations of a discrete scene $\boldsymbol{C}$, then the comparison is between a precisely defined GG output and an unspecified *approximation* of the continuous LS segmentation, and any conclusion of such effort will be only approximate. Therefore, the only precise theoretical comparison between LS and GG segmentation methods can be made at

the continuous level, that is, on the images defined on an Euclidean scene Ω. A natural approach how to relate the GG with the continuous output is described in [40].

For a continuous image $F\colon \Omega \to \mathbb{R}^k$ and a digital scene $C \subset \Omega$ let $F \restriction C$ be a digital image on C approximating F. We think about it here as a restriction of F (i.e., $(F \restriction C)(c) = f(c)$ for all $c \in C$). For a segmentation algorithm $\boldsymbol{A}$, let $\boldsymbol{A}(F \restriction C, \boldsymbol{p})$ be the output of $\boldsymbol{A}$ applied to the image $F \restriction C$ and some parameters $\boldsymbol{p}$, like seeds and cost function. We like to think of an $\boldsymbol{A}$-segmentation of the entire scene Ω of F as a result of application of $\boldsymbol{A}$ to the "image $F \restriction C$ obtained with infinite resolution." More formally, it will be understood as a limit $\boldsymbol{A}^*(F, \boldsymbol{p}) = \lim_{C\to\Omega} \boldsymbol{A}(F \restriction C, \boldsymbol{p})$ over all appropriate finite sets $C \subset \Omega$ [40]. In this set-up, we can say that a discrete segmentation algorithm $\boldsymbol{A}$ agrees (or is equivalent) at infinite resolution with a continuous (say, level set) segmentation model $\boldsymbol{M}$ in the class $\boldsymbol{F}$ of images $F\colon \Omega \to \mathbb{R}^k$ provided for every $F \in \boldsymbol{F}$ and appropriate parameter vector $\boldsymbol{p}$, the limit $\boldsymbol{A}^*(F, \boldsymbol{p})$ exists and is equal to a segmentation $\boldsymbol{M}(F, \boldsymbol{p})$ of Ω predicted by $\boldsymbol{M}$. In this sense, we have proved

Theorem 8. [40] *The FC delineation algorithm $\boldsymbol{A}_\nabla$ used with the gradient based affinity is equivalent, at infinite resolution, with a level set delineation model $\boldsymbol{M}_{LS}$ from Malladi, Sethian, and Vemuri paper [24].*

Here, the gradient based affinity is a natural discretization of a notion of gradient (see [40]) similar in spirit to the homogeneity based affinity. We should stress that there are a few hidden elements in this theorem. First of all, we consider, after the authors of [24], the outcome of the model as the viscosity solution of the propagation problem, in which the curvature parameter used in the model goes to zero. In other words, the actual outcome of the model $\boldsymbol{M}_\nabla$ does not guarantees smoothness (in a curvature sense) of the boundary. This is the only way the equivalence with GG algorithms can be achieved (at least, with the energy functions we consider), as the graphs associated with the images consist only of the first order image intensity information (the weights of edges are based on the intensities of at most two adjacent spels, which can be viewed as an approximation of the first derivative of the intensity function), while the curvature is the second order (based on the second derivative) notion, which requires information of at least three spels to be defined [16].)

The strange twist of Theorem 8 is that, in fact, it tells us nothing on the level set algorithm $\boldsymbol{A}_{LS}$, which is obtained as a discretization of the model $\boldsymbol{M}_{LS}$. Although we proved [40] that the limit $\lim_{C\to\Omega} \boldsymbol{A}_\nabla(F \restriction C, \boldsymbol{p})$ exists and is equal to $\boldsymbol{M}_{LS}(F, \boldsymbol{p})$, there is no formal prove in the literature that, for appropriate functions F, the limit $\lim_{C\to\Omega} \boldsymbol{A}_{LS}(F \restriction C, \boldsymbol{p})$ exists or that it is equal to $\boldsymbol{M}_{LS}(F, \boldsymbol{p})$. Although there are general results in the theory of differential equations indicating when a discretization of a differential equation converges to its continuous solution (in the $\boldsymbol{M}_{LS}$ case, the discrete approximation of the level set function, property (iv), can indeed converge to the

continuous level set function), such convergence implies neither the existence of the limit $\lim_{C \to \Omega} \boldsymbol{A}_{LS}(F \restriction C, \boldsymbol{p})$ nor, even if it exists, that it is equal to the continuous object indicated by the limiting surface. The story of other level sets algorithms is similar — there is a great ravine between their continuous, mathematical models and the associated discrete approximation algorithms, which should approximate the continuous models, but that are unknown (at least, theoretically) when they do so.

11.8 Medical Image Examples

The FC algorithms have been employed in segmenting medical CT, MR, and ultrasound images under various medical applications. They have also been used in non-medical image segmentation tasks. Our own application focus has been medical. These include:

- Delineation of gray matter, white matter, Cerebrospinal Fluid (CSF), lesions, diseased parts of white matter, and parcellations of these entities in different anatomic and functional regions of the brain via multi-protocol MR images for studying the multiple sclerosis disease (Fig. 11.3) and in elderly subjects to study aging related depression and dementia;
- Delineation of bone and soft tissue structures in CT images for craniomaxillofacial surgery planning (Fig. 11.4);
- Separation of arteries and veins in Magnetic Resonance Angiography (MRA) images (Fig. 11.5);
- Delineation of brain tumors in multi-protocol MR images (Fig. 11.6);

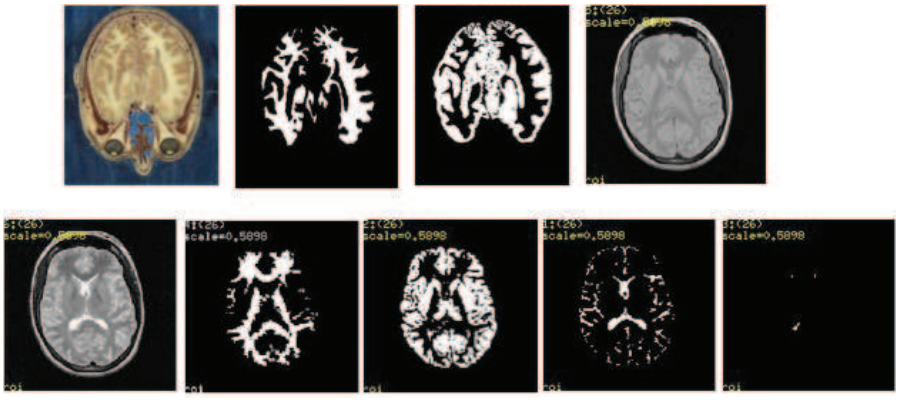

Fig. 11.3. FC and AFC segmentation of brain images. Top: Cross-sectional brain image from visible woman data set, white and gray matter segmentations via vectorial scale-based FC, and proton density weighted MRI; Bottom: T2 weighted MRI, white matter, gray matter, CSF and lesion segmentations via AFC.

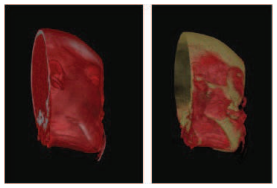

Fig. 11.4. Skin peeling via AFC segmentation. Left: Volume rendering from CT image of a patient with mid facial clefts; Right: result after skin peeling.

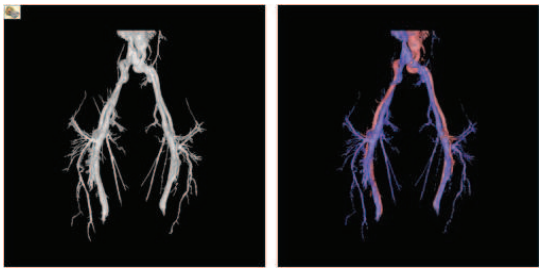

Fig. 11.5. Vessel separation via IRFC. Left: A segment of the peripheral vascular tree from MRA; Right: arteries and veins separated via IRFC.

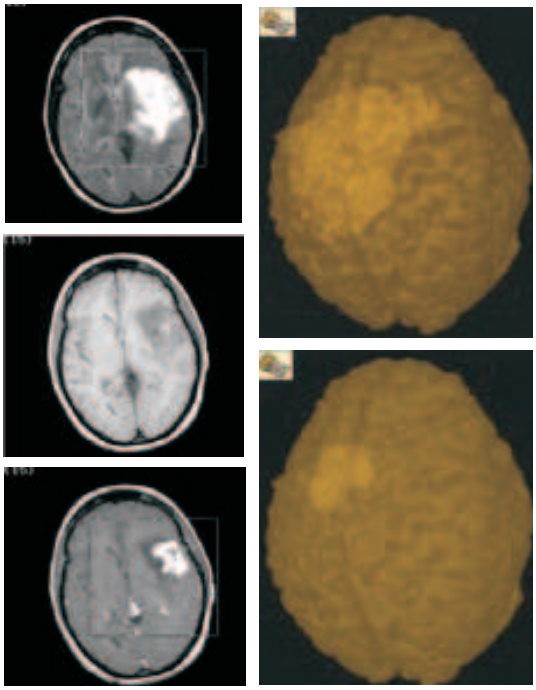

Fig. 11.6. Tumor segmentation. Left column: FLAIR and T1 weighted MRI without and with contrast agent; Right column: The edematous tumor region segmented via AFC from the FLAIR image and from the subtracted (post from pre-contrast) image showing enhancing aspects of the tumor.

- Delineation of upper airway and surrounding structures in MRI for studying pediatric Obstructive Sleep Apnea (OSA) (Fig. 11.7).

The need for image segmentation in medical applications arises from our desire to (a) characterize and quantify a disease process; (b) understand the natural course of a disease; (c) study the effects of a treatment regimen for a

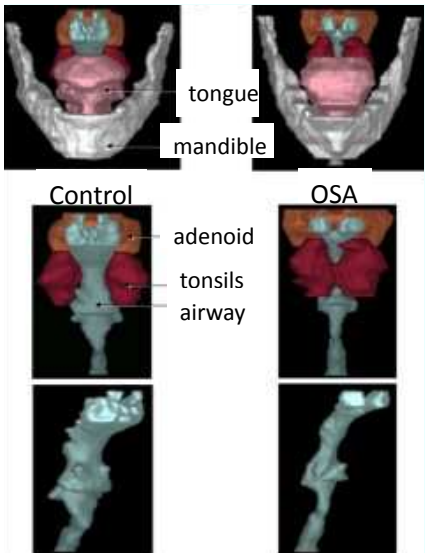

Fig. 11.7. Surface rendering of AFC-segmented MRI. Left: Upper airway and other surrounding structures (mandible, adenoid, tonsils, tongue) of a normal child; Right: a child with OSA.

disease; and (d) guide therapeutic procedures. In our applications, the motivation came from (a)-(c). The performance of the different FC algorithms has been evaluated in these applications quite extensively; please refer to the specific application related papers cited in [41]. The reasons for choosing FC in these applications are mainly three-fold. (1) We are intimately familiar with the FC technology, have the full resources of its implementation, and have the expertise for optimally utilizing them in medical applications. These are crucial requirements for the optimal use of any segmentation algorithm. (2) Among comparable other families of algorithms (such as graph cuts, watershed, level sets), FC constitutes one of the fastest groups of algorithms. (3) The FC formulation is entirely digital starting from first principles, and so there are no ad hoc/unspecified continuous-to-digital conversion issues.

11.9 Concluding Remarks

Focusing mainly on FC methods, we have presented a unified mathematical theory wherein four currently predominant, purely image-based approaches – GC, WS, LS, and FC – are described in a single framework as energy optimization methods in image segmentation. Among these, LS has a continuous formulation and poses some challenges, unenunciated in the literature, on how to reconcile it with the eventual computational/algorithmic requirements of discretization. The remaining – GC, WS, FC – have an inherently discrete formulation and lend themselves naturally to combinatorial optimization solutions. The unifying treatment has helped us in delineating the similarities

and differences among these methods and in pinpointing their strengths and weaknesses.

All segmentation methods rely on a (local) attribute functional of some sort – we called them affinity for FC and edge cost in general – for transforming intensity information into contributions to the energy functional. The notion of equivalent affinities is useful in characterizing the distinct and unique aspects of this function that have a real impact on the energy functional. Such an analysis can also be carried out for the attribute functionals of GC, WS, and LS, and of any other segmentation methods, although this does not seem to have been done. (But compare [35].) Its consequence on nailing down the real independent parameters of a segmentation algorithm has implications in setting the segmentation algorithm optimally for a given application domain and in evaluating its robustness to parameter settings.

In all FC developments so far, for theoretical and algorithmic simplicity, only 2-ary fuzzy relations have been considered (meaning, affinity and connectedness have been considered only between two spels). Further, in the composition of fuzzy relations such as ψ_σ and ϕ_σ (for a given object and for all objects), only union and max-min constructs have been employed for the same reasons. Relaxing these restrictions may lead to new, more powerful and effective algorithms. For example, m-ary relations can be defined by considering all spels in the local scale region. Further, considering fuzzy relations as both fuzzy subsets of the scene and as m-ary relations ($m \geq 2$), various fuzzy subset operations (such as algebraic union, product, etc.) and compositing operations (such as max-star, sum-min, sum-product, algebraic-sum-min, etc.) can also be used. Prior object shape and appearance fuzzy models can also be brought into this realm. These require considerable theoretical, algorithmic, and application related work.

References

1. Udupa JK, Samarasekera S. Fuzzy connectedness and object definition: theory, algorithms, and applications in image segmentation. Graph Models Image Process. 1996;58(3):246–261.
2. Saha PK, Udupa JK. Relative fuzzy connectedness among multiple objects: theory, algorithms, and applications in image segmentation. Comput Vis Image Underst. 2001;82(1):42–56.
3. Udupa JK, Saha PK, Lotufo RA. Relative fuzzy connectedness and object definition: theory, algorithms, and applications in image segmentation. IEEE Trans Pattern Anal Mach Intell. 2002;24:1485–1500.
4. Saha PK, Udupa JK. Iterative relative fuzzy connectedness and object definition: theory, algorithms, and applications in image segmentation. Proc IEEE Workshop Math Methods Biomed Image Anal. 2002; p. 28–35.
5. Ciesielski KC, Udupa JK, Saha PK, et al. Iterative relative fuzzy connectedness for multiple objects, allowing multiple seeds. Comput Vis Image Underst. 2007;107(3):160–182.

6. Zhuge Y, Udupa JK, Saha PK. Vectorial scale-based fuzzy connected image segmentation. Comput Vis Image Underst. 2006;101:177–193.
7. Carvalho BM, Gau CJ, Herman GT, et al. Algorithms for fuzzy segmentation. Pattern Anal Appl. 1999;2:73–81.
8. Herman GT, Carvalho BM. Multiseeded segmentation using fuzzy connectedness. IEEE Trans Pattern Anal Mach Intell. 2001;23:460–474.
9. Carvalho BM, Herman GT, Kong YT. Simultaneous fuzzy segmentation of multiple objects. Discrete Appl Math. 2005;151:65–77.
10. Pednekar A, Kakadiaris IA. Image segmentation based on fuzzy connectedness using dynamic weights. IEEE Trans Image Process. 2006;15(6):1555–1562.
11. Fan X, Yang J, Cheng L. A novel segmentation method for MR brain images based on fuzzy connectedness and FCM. Lect Notes Computer Sci. 2005;3613:505–513.
12. Boykov Y, Veksler O, Zabih R. Fast approximate energy minimization via graph cuts. IEEE Trans Pattern Anal Machine Intell. 2001;23(11):1222–1239.
13. Boykov Y, Jolly M. Interactive graph cuts for optimal boundary & region segmentation of objects in N-D images. Proc ICCV. 2001;I:105–112.
14. Boykov Y, Kolmogorov V. Computing geodesics and minimal surfaces via graph cuts. Proc ICCV. 2003;I:26–33.
15. Boykov Y, Kolmogorov V. An experimental comparison of min-cut/max- flow algorithms for energy minimization in vision. IEEE Trans Pattern Anal Mach Intell. 2004;26:1124–1137.
16. Boykov Y, Funka-Lea G. Graph cuts and efficient N-D image segmentation. Int J Computer Vis. 2006;70:109–131.
17. Boykov Y, Kolmogorov V, Cremers D, et al. An integral solution to surface evolution PDEs via geo-cuts. Lect Notes Comp Sci. 2006;3953:409–422.
18. Boykov Y, Veksler O. Graph cuts in vision and graphics: theories and applications. In: Paragios N, Chen Y, Faugeras O, editors. Handbook of Mathematical Models and Computer Vision. Springer-Verlag; 2006. p. 79–96.
19. Shi J, Malik J. Normalized cuts and image segmentation. IEEE Trans Pattern Anal Mach Intell. 2000;22:888–905.
20. Miranda PAV, Falcao AX. Links between image segmentation based on optimum-path forest and minimum cut in graph. J Math Imaging Vis. 2009;35:128–142.
21. Beucher S. The watershed transformation applied to image segmentation. Proc 10th Pfefferkorn Conf Signal Image Process Microsc Microanal. 1992; p. 299–314.
22. Shafarenko L, Petrou M, Kittler J. Automatic watershed segmentation of randomly textured color images. IEEE Trans Image Process. 1997;6:1530–1544.
23. Park J, Keller J. Snakes on the watershed. IEEE Trans Pattern Anal Mach Intell. 2001;23:1201–1205.
24. Malladi R, Sethian J, Vemuri B. Shape modeling with front propagation: a level set approach. IEEE Trans Pattern Anal Mach Intell. 1995;17:158–175.
25. Sethian JA. Fast Marching Methods and Level Sets Methods. Evolving Interfaces in Computational Geometry, Fluid Mechanics, Computer Vision, and Materials Science. Cambridge Univ. Press; 1999.
26. Saha PK, Udupa JK, Odhner D. Scale-based fuzzy connectedness image segmentation: theory, algorithms, and validation. Computer Vis Image Underst. 2000;77:145–174.

27. Falcao AX, Stolp J, Lotufo RA. The image foresting transform: theory, algorithms, and applications. IEEE Trans Pattern Anal Mach Intell. 2004;26(1):19–29.
28. Ciesielski KC, Udupa JK. Affinity functions in fuzzy connectedness based image segmentation II: defining and recognizing truly novel affinities. Computer Vis Image Underst. 2010;114:155—166.
29. Saha PK. Tensor scale: a local morphometric parameter with applications to computer vision and image processing. Computer Vis Image Underst. 2005;99:384–413.
30. Ciesielski K. Set Theory for the Working Mathematician. No. 39 in London Mathematical Society Students Texts. Cambridge University Press; 1997.
31. Ciesielski KC, Udupa JK. Affinity functions in fuzzy connectedness based image segmentation I: equivalence of affinities. Computer Vis Image Underst. 2010;114:146—154.
32. Rosenfeld A. Fuzzy digital topology. Inf Control. 1979;40:76–87.
33. Rosenfeld A. On connectivity properties of grayscale pictures. Pattern Recognit. 1983;16:47–50.
34. Rosenfeld A. The fuzzy geometry of image subsets. Pattern Recognit Lett. 1984;2:311–317.
35. Kolmogorov V, Zabih R. What energy functions can be minimized via graph. IEEE Trans Pattern Anal Mach Intell. 2004;26(2):147–159.
36. Audigier R, Lotufo RA. Duality between the watershed by image foresting transform and the fuzzy connectedness segmentation approaches. Proc 19th Brazilian Symposium Comput Graph Image Process. 2006;.
37. Kass M, Witkin A, Terzopoulos D. Snakes: active contour models. Int J Comput Vis. 1987;1:321–331.
38. Mumford D, Shah J. Optimal approximations by piecewise smooth functions and associated variational problems. Commun Pure Appl Math. 1989;42:577–685.
39. Chan TF, Vese LA. Active contours without edges. IEEE Trans Image Process. 2001;10:266–277.
40. Ciesielski KC, Udupa JK. A general theory of image segmentation: level set segmentation in the fuzzy connectedness framework. Proc SPIE. 2007;6512.
41. Udupa JK, Saha PK. Fuzzy connectedness in image segmentation. Proc IEEE. 2003;91:1649–1669.